J Nanostruct 16(1): 988-994, Winter 2026

RESEARCH PAPER

Preparation of Chili Pepper-Derived Nanocomposites and Study of Some of Their Physical and Biological Applications

Wisam Mahmood Mohammed [1], Aws K. Mohammed [2], Ahmed M. Shano [3]*

[1] *Ministry of Education, Open Educational College, Iraq*

[2] *Ministry of Education, General Directorate of Education in Diyala, Iraq*

[3] *Department of Radiological Techniques, Bilad Alrafidain University College, Diyala, Iraq*

ARTICLE INFO

Article History:
Received 04 October 2025
Accepted 07 December 2025
Published 01 January 2026

Keywords:
Bacteria
Capsaicin
FTIR
SEM
XRD

ABSTRACT

Medicinal plants: They are characterized as plants that, when given to a patient in their pure form or after extraction, have the physiological capacity to treat a particular disease or, at the very least, lower its incidence. These plants contain one or more chemical substances in one or more of their various organs in high or low concentration. Thus, capsaicin extract, which is present in spicy peppers,found in cloves, were chosen as antibacterial substances for some types of bacteria. This study included the preparation of new nano composite of extracted capsaicin. The prepared compounds characterized using infrared spectroscopy FTIR, XRD, SEM, the biological effectiveness of compounds will study against different types of bacteria and fungi.

How to cite this article
Mahmood Mohammed W., Mohammed A., M. Shano A. Preparation of Chili Pepper-Derived Nanocomposites and Study of Some of Their Physical and Biological Applications. J Nanostruct, 2026; 16(1):988-994. DOI: 10.22052/JNS.2026.01.088

INTRODUCTION

A host of new and improved products is produced for various applications. Richard Feynman physicist [1] introduced the concept of nanotechnology in 1959 in his talk "There "'s Plenty of Room at the Bottom." „Nano science" is a compound term made up of the words science and nano, which imply "dwarf." One billionth of a meter, or 10-9, is referred to as a nanometer. Human hair, in contrast, has a thickness of 100,000 nm. The study of materials and technology in the 1-100 nm scale is known as nanoscience. Any material will exhibit significant changes in its basic electrical and optical characteristics along with a reduction in size when the thermal energy (kT) is exceeded by the energy separation between electronic levels. The electronic energy levels of tiny nanocrystals are the result of the electronic wave function being constrained to the particle's physical size [2-3] Because of this phenomenon, which is known as quantum confinement, quantum dots (QDs) are another name for nanocrystals. Once the particle's diameter equals the electron wave function's wavelength, the quantum confinement effect may be seen. The electrical and optical characteristics of the materials differ significantly from those of bulk materials when they are so tiny. A particle acts in the same way as Because they differ from macroparticles in terms of their chemical and physical characteristics, nanoparticles are unique and fascinating. Gold nanoparticles are one type of nanoscale example of the surface area to volume ratio. While gold is an

* *Corresponding Author Email: mahmoodwisam737@gmail.com*

inert element at the macroscale, meaning it does not react with many substances, gold nanoparticles become highly reactive at the nanoscale and can be employed as catalysts to accelerate reactions [4-5]. Particle size has an impact on gold's chemical activity. Only gold nanoparticles with a diameter of less than 5 nm are known to exhibit catalytic activity. Small particles have a disproportionately high quantity of poorly coordinated. It is known that polymer nanocomposites are a type of reinforced polymer in which there are extremely few nanometric clay particles, less than five percent. These materials received a great deal of interest at the same time from academic institutions and industry, particularly in the field of nanocomposites [6]. This can be attributed to their significantly better thermal, mechanical, and barrier qualities as compared to conventional and micro-composite materials. Notable differences between these materials include enhanced thermal stability and fire resistance, better barrier qualities, and higher recyclability. many applications for polymer nanocomposites, regardless of the industry in which they are employed. Golf balls and other hybrids constructed of poly rubber (dimethyl siloxane) and nanosilica can be given a precise shape by hydrolyzing tetraethyl-ortho-silicate. They are composed of inorganic particles with dimensions ranging from 1 to 100 nm and biopolymers. They have a wide range of applications because of their multifaceted qualities, which include antibacterial activity, biocompatibility, and biodegradability. The significant decrease in the use of fossil fuels is the practical result of the increased demand for bio-based polymers. Because they are biocompatible, they are advantageous for use in biomedical applications as well as cosmetics and biotechnology. They will be crucial in the future as environmentally friendly, sustainable materials. [7, 8]. Bio-nanocomposites will replace the petroleum-based polymer that is now in use.

MATERIALS AND METHODS

Materials

Ferric nitrite. To prevent the agglomeration of the nanoparticles, we used polyvinyl alcohols (PVA, MW = 88000–96800, degree of polymerization = 2000–2200) as stabilizer and polymer nanocomposite matrix. Copper (II) sulfate pentahydrate ($CuSO_4.5H_2O$) (Riedel-de Haen AG. maleic anhydride (Fluka Company. Polyvinyl alcohols (In order of sp) were used from fluka company. 9H2O was used. All chemicals were used as is without any processing upon receipt.

Procedure

A (0.008mol, 2 gm) of chili pepper was dissolved in (8) ml of (0.5% N) sodium hydroxide, (6ml) of DMF. The mixture was then supplemented with (1.3) grams of maleic anhydride. For four hours, the mixture was heated to 70 °C in a water bath while being agitated. The thick red oily substance was gathered, and any leftover materials were cleaned with 10 milliliters of diethyl ether. The products were filtered and dried in a vacuum oven at 60 °C overnight [8].

Copper oxide nanoparticles preparation

Copper-oxide-NPs are prepared by the hydrothermal route. In beaker A, we mix 2g of Copper (II) Sulfate $CuSO_4.5H_2O$ with 0.5g of hexamethylenetetramine (HMT) $[(CH_2).6N_4]$. The contents of beaker A were dissolved in 50ml of distilled water of pH eight. The mixture is then heated at 90 °C for five hours to produce powder CuO-NPs. CuO-NPs were heated for 24 h at a temperature range of 60-70 °C after centrifugation. Distilled water was used to purge the CuO-NPs three times to remove impurities and residues. After obtaining CuO-NPs in powder form, they were heated with a furnace at 400 °C for 2 hours.

Preparation Process of PVA/Chili Pepper-g-Maleate with CuO NPs [H1] doped

The glass substrates underwent a multistep cleaning procedure prior to use. Gross contaminants were first removed by washing with heated tap water. This was followed by organic residue elimination through acetone treatment and subsequent rinsing with ionized water adjusted to an acidic pH (3.5). Final purification was achieved by sonication in distilled water for 5 minutes, after which the substrates were air-dried using a cold airflow. One gram of chili pepper-g- maleate and one gram of PVA are dissolved in 200 ml (1:1) ethanol: dioxin. The preparation of (chili pepper-g-maleate -PVA) solution consists of mixing both (chili pepper-g- maleate and PVA) solutions in a volume ratio of 1:1 for 24 hours under magnetic stirring for uniformity. The prepared suspension was first passed through a membrane filter (0.45 µm, Millipore) and subsequently deposited onto glass substrates using the dip-coating technique. All nanocomposite synthesis steps were carried out

under ambient conditions at 27 °C and atmospheric pressure. At the nanoscale, CuO nanoparticles were effectively stabilized within the PVA matrix through organic surface modification mediated by the starch-based polymer component. Before coating, the final sols were additionally purified using a paper filter with a pore size of 0.40 µm. The sol–gel solutions exhibited viscosities in the range of 1.2079–2.8935 cP.

Uniform thin films of (chili pepper-g-maleate-PVA)/CuO nanocomposites were fabricated by dip-coating onto glass substrates, yielding films with an average thickness of approximately 500 nm and a maximum thickness variation of 7.5%. The overall coating process required approximately two hours. Film thickness and surface morphology were evaluated using scanning electron microscopy (SEM). Following deposition, the coated substrates were thermally treated at 70 °C for 15 min to facilitate solvent evaporation and remove residual organic species.

Structural characterization was conducted by X-ray diffraction analysis over a scanning range of 10–80° at a constant scan rate. Functional group interactions and chemical bonding within the nanocomposite films were investigated using Fourier-transform infrared (FTIR) spectroscopy.

Preparation composite of chili pepper-g- maleic anhydride

To produce Fe_3O_4 NPsIron nitrate and sodium chloride were dissolved in deionized water at molar ratios of 1:50 and 1:20, respectively. Uniform solid solution was produced in the mixture during stirring at 70 °C drying. The NPs were created through solid salt annealing of about 30 min in a tube furnace at 700 °C and cooled naturally at room temperature. To remove sodium chloride, the product was washed with deionized water and then oven dried at 60 °C. To avoid the agglomeration of the NPs and modify their surface chemistry, the 1 wt% solution of chili pepper-g- maleic anhydride- g-polyvinyl alcohol aqueous was applied to the as-synthesized NPs immediately after annealing. The de-ionized water was used to wash off the NaCl from the particles. The agglomerated Fe_2O_3 NPs were dispersed in the desired quantity in a 5 wt% aqueous solution (20 mL) of copolymer (chili pepper-g-maleate-polyvinyl alcohol) to obtain the polymer nanocomposite materials. The solution of iron oxide nanoparticles (chili pepper-g-maletat and polyvinyl alcohol) was cast in a petri dish and was completely dried at 60 °C.

RESULTS AND DICUSSION

FTIR ANALYSIS

This part included the preparation of new graft polymer of chili pepper-g- maletat -PVA. The infrared spectra of the compounds (H1, H2), Figs. 1 and 2 respectively, explain the existence of a band in the range of (3322-3188) cm^{-1}, which refers to the stretching vibrations of hydroxyl groups. The spectra of these compounds show bands at the range of (3105- 3000) cm^{-1} due to (C-H)Aromatic., and shows two bands in the range of (2989- 2844) cm^{-1} due to (C-H)Aliphatic [8] these compounds appeared as bands in the range of (1687) cm^{-1} which belongs to (C = O) ester, and 1726) cm^{-1} which

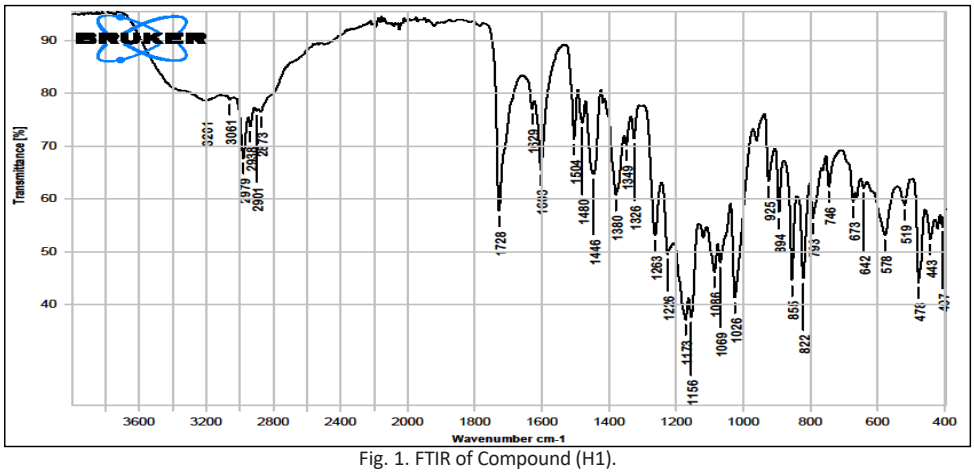

Fig. 1. FTIR of Compound (H1).

belongs to (C = O) carboxylic. The (C=C) bending appeared at (1458-1433) cm^{-1} of the spectrum. The reason for the band's strength in all nanocomposite samples is the C-O group's stretching mode. The two prominent bands were seen at approximately 1418 cm^{-1}. The stretching and bending modes of the CH_2 group are responsible for the two strong bands visible at around 1418 cm^{-1} and 842 cm^{-1}, respectively. Meanwhile, the curving of the (phenolic) OH group is displayed by a minor crest located at 1380.89 cm^{-1}. Furthermore, because to the notable expansion of the M-O-C bond at 678

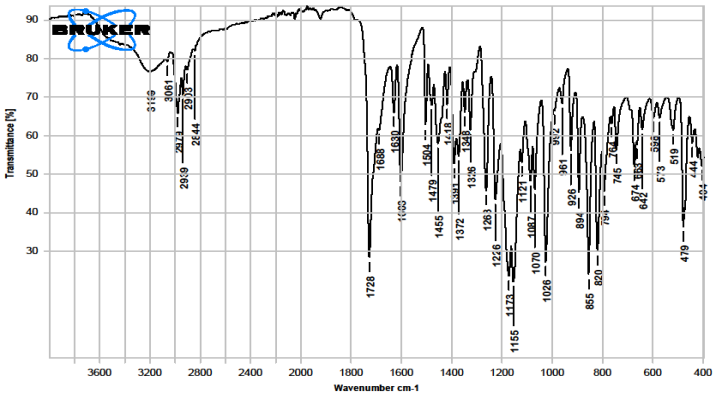

Fig. 2. FTIR of Compound (H2).

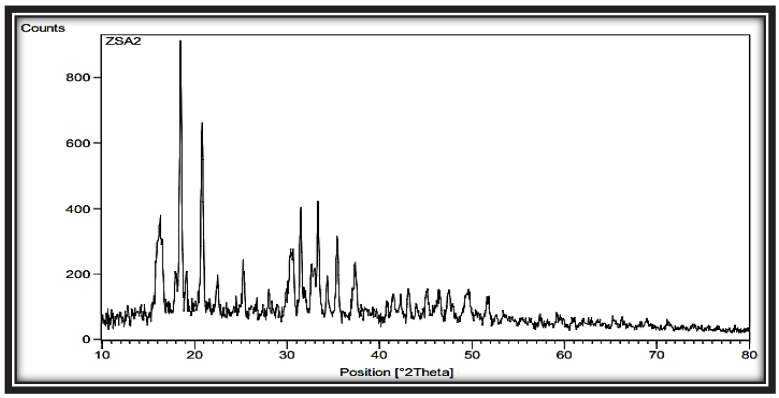

Fig. 3. XRD patterns of FeO Nanocomposite.

Fig. 4 – XRD patterns of CuO Nanocomposit

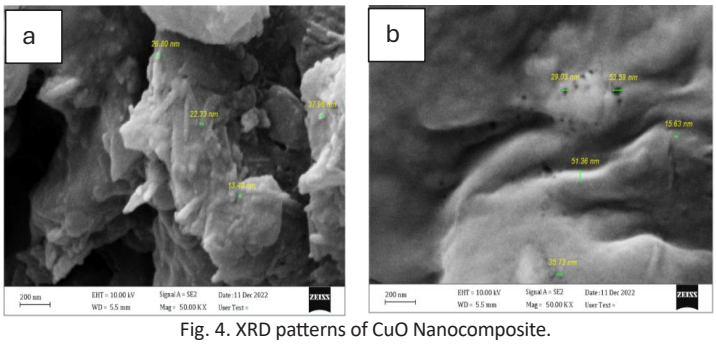

Fig. 4. XRD patterns of CuO Nanocomposite.

cm^{-1}, 678 cm^{-1} attributed to FeO and CuO two peaks, 1097.5 cm^{-1} and 1136.07 cm^{-1}, may be seen in the region of 1100 cm^{-1} [11, 12]. The spectrum of (chili pepper-g- maleate -PVA) CuO-NPs The spectrum of (chili pepper-g- maleate -PVA) CuO-NPs - showed two bands at 894, 315, and 229 nm (11186, 31746, and 43668) cm^{-1}, The spectrum of(chili pepper-g-maleate -PVA) FeO-NPs showed three bands at 701, 590, and 339 nm (14265, 16949), [13,14].

X-Ray diffraction assessment

X-ray techniques were employed to investigate the structural characteristics of the synthesized nanoparticles. X-ray diffraction (XRD) measurements were carried out for the Schiff base ligand complexes. The diffraction patterns of FeO and CuO exhibited broadened reflections, confirming the formation of materials at the nanoscale. Several diffraction features were detected at 2θ values of approximately 16, 18.5, 21, 25, 30.5, 32, 34, 35.5, and 37.5°; however, these peaks appeared weak and poorly resolved. The loss of well-defined diffraction signals is attributed to the shielding or encapsulation effect of the polymeric ligand molecules, which likely suppresses crystal plane resolution in X-ray analysis, as illustrated in Figs. 3 and 4.

The sharp peaks that appear in all complexes confirm that the particles of these complexes are in the nano range. The crystallite size was determined by using Debye-Scherer'se equation [15-20]:

where θ is the diffraction angle, β the full width at half maximum (FWHM), D the crystallite size and λ the wavelength of the X-ray photons (λ = 0.15406 nm).

Scanning Electron Microscopy (SEM)

The CuO nano composites were examined under

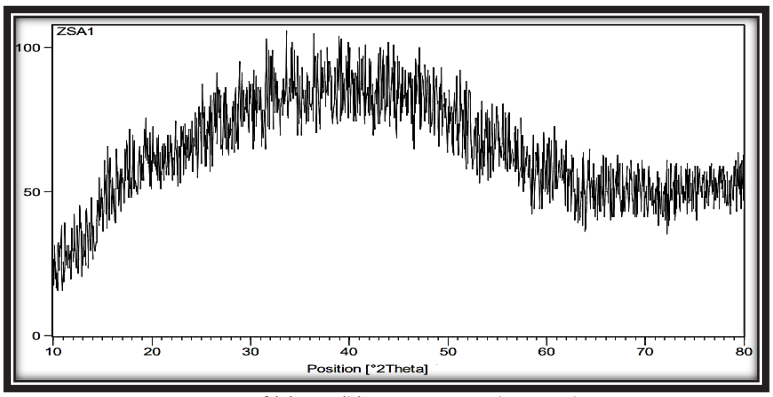

Fig. 5. SEM of (a) CuO (b) FeO nanoparticles complexes.

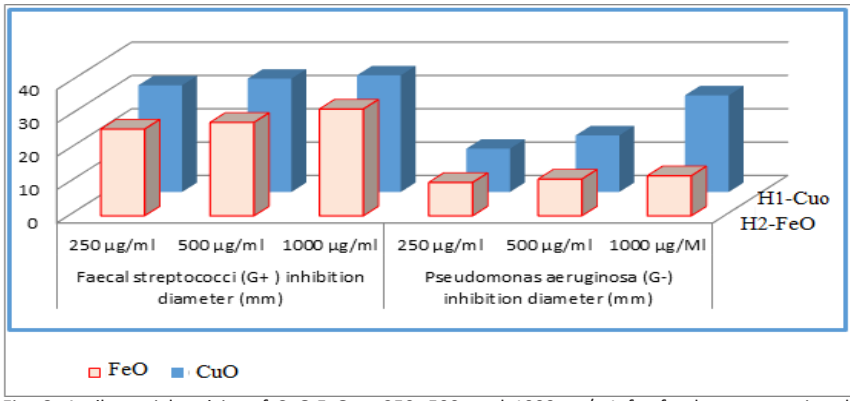

Fig. 6. Antibacterial activity of CuO,FeO at 250, 500, and 1000 µg/mL for fecal streptococci and Pseudomonas aeruginosa.

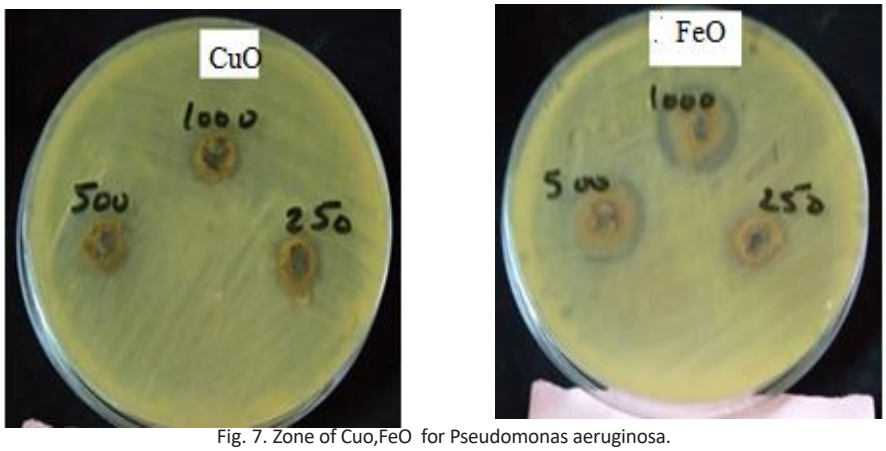

Fig. 7. Zone of Cuo,FeO for Pseudomonas aeruginosa.

Table 1. The effectiveness of bacteria against the prepared compounds (H1-CuO, H2- FeO.

Compound	Fecal streptococci (G+) inhibition diameter (mm)			Pseudomonas aeruginosa (G-) inhibition diameter (mm)		
	250 µg/ml	500 µg/ml	1000 µg/ml	250 µg/ml	500 µg/ml	1000 µg/ml
H1 - CuO	23	25	32	12	13	16
H2 FeO	35	37	36	19	20	29

a scanning electron microscope (SEM), which showed the size ranging from about 15-51 nm (10). FrO nano composite was similar in this respect. Moreover, scanning electron microscopy (SEM) images reveal that particle sizes are around 13-37 nm [21]. Fig. 5 has relevant details.

Biological Activity of Chili Pepper

Candida albicans is caused by the human fungal pathogen that causes candidiasis. Candida albicans is a pathogenic yeast in the human intestinal microbiota with antifungal properties. The organism can also survive outside of the human body. Analysis of anti-fungal activities against Candida albicans in three different concentrations of the nanocomposite showed moderate to good anti-fungal activity (3-26) Table 1. The antibacterial activity of these compounds was studied against Staphylococcus and Escherichia coli, which were tested (in vitro). In the reference agar diffusion technique at a concentration of (1 ppm), no obvious change in the growth of bacteria was observed, so DMSO was used, and the plates were incubated at (37°C) for (24 hours). The measurements were taken in mm, and results are in Table 1, which showed that all of the compounds had a more growth inhibition zone diameter and showed slight activity against Candida albicans than bacteria inhibition [22] as shown in Figs. 6 and 7.

CONCLUSION

This study included the preparation of new nano composite of extracted chili pepper. The prepared compounds characterized using infrared spectroscopy FTIR, XRD. SEM, the biological effectiveness of compounds will study against different types of bacteria and fungi.

CONFLICT OF INTEREST

The authors declare that there is no conflict of interests regarding the publication of this manuscript.

REFERENCES

1. Li H-Z, Chen S-C, Wang Y-Z. Preparation and characterization of nanocomposites of polyvinyl alcohol/cellulose nanowhiskers/chitosan. Composites Science and Technology. 2015;115:60-65.
2. DOI reserve for Community Guide 004. Centers for Disease Control and Prevention; 2024 2024/10/07.
3. Gonzalez JS, Nicolás P, Ferreira ML, Avena M, Lassalle VL, Alvarez VA. Fabrication of ferrogels using different magnetic nanoparticles and their performance on protein adsorption. Polym Int. 2013;63(2):258-265.
4. Ponappa K, Aravindan S, Rao PV, Ramkumar J, Gupta M. The effect of process parameters on machining of magnesium nano alumina composites through EDM. The International Journal of Advanced Manufacturing Technology. 2009;46(9-12):1035-1042.
5. Thomas DJ. Developing nanocomposite 3D printing filaments for enhanced integrated device fabrication. The International Journal of Advanced Manufacturing

Technology. 2018;95(9-12):4191-4198.
6. Torimoto T. Nanostructure Engineering of Size-Quantized Semiconductor Particles for Photoelectrochemical Applications. Electrochemistry. 2017;85(9):534-542.
7. Shi Y, Xiong DS, Peng Y, Wang N. Effects of polymerization degree on recovery behavior of PVA/PVP hydrogels as potential articular cartilage prosthesis after fatigue test. Express Polymer Letters. 2016;10(2):125-138.
8. An X, Yang X, Dong W, Ni C, Jiang X, Li X. Synthesis and fouling resistance of capsaicin derivatives containing amide groups. Chem Phys Lett. 2022;803:139824.
9. Rani J, Sharma A, Vishnoi R, Yadav S. Concept of Prativisha: An Unmapped Area. International Journal of Ayurveda and Pharma Research. 2023:72-75.
10. Jayaprakash J, Srinivasan N, Chandrasekaran P. Surface modifications of CuO nanoparticles using Ethylene diamine tetra acetic acid as a capping agent by sol–gel routine. Spectrochimica Acta Part A: Molecular and Biomolecular Spectroscopy. 2014;123:363-368.
11. Ali IM, Shano AM, Bakr NA. H2S gas sensitivity of PAni nano fibers synthesized by hydrothermal method. Journal of Materials Science: Materials in Electronics. 2018;29(13):11208-11214.
12. Abd AN, Ismail RA, Habubi NF. Characterization of CdS nanoparticles prepared by laser ablation in methanol. Journal of Materials Science: Materials in Electronics. 2015;26(12):9853-9858.
13. Mahmood S, Mei TS, Yee WX, Hilles AR, Alelwani W, Bannunah AM. Synthesis of Capsaicin Loaded Silver Nanoparticles Using Green Approach and Its Anti-Bacterial Activity Against Human Pathogens. J Biomed Nanotechnol. 2021;17(8):1612-1626.
14. Ahmady AR, Solouk A, Saber-Samandari S, Akbari S, Ghanbari H, Brycki BE. Capsaicin-loaded alginate nanoparticles embedded polycaprolactone-chitosan nanofibers as a controlled drug delivery nanoplatform for anticancer activity. Journal of Colloid and Interface Science. 2023;638:616-628.
15. Shano AM, Ali ZS. Fabrication and Characterization of Polyaniline Nanofiber Films by Various Techniques. Journal of Nano- and Electronic Physics. 2020;12(4):04001-04001-04001-04005.
16. Khudhur AM, Shano AM, Abbas ASH. A New Neuron Ion Channel Model Under Time Varying Input Currents. Journal of Physics: Conference Series. 2021;1999(1):012127.
17. Mahi K, Ait-Kaci H. A Novel Analytical Approach to the Solar Cell Junction Physical Parameters Identification. Journal of Nano- and Electronic Physics. 2023;15(6):06016-06011-06016-06015.
18. Khodair ZT, Al-Jubbori MA, Shano AM, Sharrad FI. Study of Optical and Structural Properties of $(NiO)_{1-x}(CuO)_x$ Nanostructures Thin Films. Chemical Data Collections. 2020;28:100414.
19. Ali ZS, Shano AM. The Influence of Solvents on Polyaniline Nanofibers Synthesized by a Hydrothermal Method and their Application in Gas Sensors. J Electron Mater. 2020;49(9):5528-5533.
20. Jasim SK, Shano AM, Adnan SK. Zinc Oxide Poly Crystals Heterojunction and Infrared- Blind UV-Photodetector. Journal of Nano- and Electronic Physics. 2024;16(1):01012-01011-01012-01016.
21. Batiha GE-S, Alqahtani A, Ojo OA, Shaheen HM, Wasef L, Elzeiny M, et al. Biological Properties, Bioactive Constituents, and Pharmacokinetics of Some Capsicum spp. and Capsaicinoids. Int J Mol Sci. 2020;21(15):5179.
22. Awad IMA, Hassan KM. Studies in Vilsmeier-Haack reaction. Application to quinoxalinones. Collection of Czechoslovak Chemical Communications. 1990;55(11):2715-2721.